



Foveal structure, function and microvascular morphology in school-age children with laser-treated retinopathy of prematurity

Zhiqiao Liang¹ · Yuou Yao¹ · Guosheng Sun¹ · Mingwei Zhao¹ · Hong Yin¹

Received: 23 November 2019 / Revised: 28 July 2020 / Accepted: 31 July 2020 / Published online: 10 August 2020
© The Author(s), under exclusive licence to The Royal College of Ophthalmologists 2020

Abstract

Purpose The purpose of this retrospective case-control study was to evaluate the relationship between foveal structure, function, microvascular morphology and visual acuity in school-age children with laser-treated retinopathy of prematurity (ROP).

Methods Foveal structural parameters, including the central foveal thickness (CFT), inner retinal thickness (IRT) and outer retinal thickness (ORT), were measured on B-scans using an Optovue XR Avanti optical coherence tomography device. Foveal microvascular parameters, including the foveal avascular zone (FAZ), superficial capillary plexus-vessel density (SCP-VD) and deep capillary plexus-vessel density (DCP-VD), were measured on optical coherence tomography angiography with a scan size of 3 × 3. The P1 amplitudes and P1 implicit times were recorded by a multifocal electroretinogram with 61 elements.

Results Fifty-five eyes (26 eyes of school-age ROP children and 29 eyes of full-term controls) were analysed. The ROP children manifested a significantly smaller FAZ, higher SCP-VD and higher DCP-VD than the controls ($p < 0.001$). The CFT ($p < 0.001$), IRT ($p < 0.001$) and ORT ($p = 0.001$) were significantly increased in the ROP group. The P1 amplitudes in all five-ring retinal regions were significantly smaller in the ROP group ($p < 0.001$). Multivariable analysis indicated that best-corrected visual acuity was positively correlated with post-menstrual age (PMA) and negatively correlated with SCP-VD and CFT ($R^2 = 0.529$, $p < 0.001$, 0.043 and 0.020, respectively).

Conclusion The foveal structure, function and microvascular morphology are affected in school-age children with laser-treated ROP. PMA, foveal structural anomalies and microvascular changes in ROP children were associated with impaired visual function.

Introduction

Retinopathy of prematurity (ROP) is classified as a vasoproliferative disorder and can affect the central retina, which can lead to impaired visual acuity and visual sensitivity [1, 2]. The central macula contributes to the

excellent visual acuity of healthy adults, and the development is protracted until several years after birth [3, 4]. Children born preterm have an increased risk of macular development delay [5].

Recent studies have reported that optical coherence tomography (OCT) can reveal several microstructural abnormalities, including increased central foveal thickness (CFT) and retention of inner retinal layers at the foveal centre [3, 6–9]. Optical coherence tomography angiography (OCTA) is a fast method for visualising blood vessels layer by layer within the macula without the need for dye injection. A few studies have focused on foveal microvascular abnormalities in school-age children with ROP by OCTA [10–13]. Multifocal electroretinogram (mfERG) responses are generated from cone-driven bipolar cells under light-adapted conditions [14]. The amplitudes and implicit times of the central ring can reflect the function of the fovea. Previous studies have indicated that central retinal function

Supplementary information The online version of this article (<https://doi.org/10.1038/s41433-020-01127-z>) contains supplementary material, which is available to authorized users.

✉ Hong Yin
dr_yinhong@163.com

¹ Department of Ophthalmology, Peking University People's Hospital, Eye Diseases and Optometry Institute, Beijing Key Laboratory of Diagnosis and Therapy of Retinal and Choroid Diseases, College of Optometry, Peking University Health Science Center, Beijing, China

was impaired in school-age children with ROP compared to children born at term using mfERG. OCT, OCTA and mfERG were applied to evaluate microstructural abnormalities, microvascular anomalies and local retinal function, respectively. The relationship between the foveal structure, vascular morphology and function and the correlation with visual acuity have yet to be well discussed. This study aimed to correlate visual acuity with foveal structure, function and microvascular morphology in school-age children with laser-treated ROP.

Methods

Subjects

In this observational case series, all children with ROP had a history of laser photocoagulation who were followed up in the Department of Ophthalmology of Peking University People's Hospital from July 1, 2018, to August 1, 2018. During the neonatal period, these children were screened by an experienced ophthalmologist. Two experienced ophthalmologists confirmed the zone, stage and presence of plus sign by binocular indirect ophthalmoscopy examination, which was important for treatment decisions. All the children received laser photocoagulation within 2 days after diagnosis of ROP without further intravitreal injection of anti-vascular endothelial growth factor (anti-VEGF) agents or surgery and successfully regressed during follow-up. The control group ($n = 29$) included children born at full term and matched according to age and sex and with no evidence of ocular pathology in either eye. The control subjects visited our clinic for refractive error. The exclusion criteria of the current study were as follows: (1) any previous intravitreal injection of other anti-VEGF agents, laser photocoagulation, cryotherapy or surgical procedure; (2) substandard-quality OCT, OCTA or mfERG scans resulting from low transparency of ocular media, fixation loss to the target light or poor electrode contact and (3) the presence of any other neurologic or ocular disorders that could possibly affect the results.

All subjects received a complete ophthalmologic examination consisting of best-corrected visual acuity (BCVA), spherical equivalent (SE), orthoptic assessment, anterior segment examinations and binocular indirect ophthalmoscopy examination. At the clinical examination, each participant was considered to have a normal macula detected by binocular indirect ophthalmoscopy examination. For the statistical analysis, the Snellen BCVA was converted to the logarithm of the minimum angle of resolution (logMAR). Cycloplegic refraction (0.5% tropicamide and 0.5% phenylephrine) was recorded as sphere, cylinder and axis representing the SE.

Approval from the Ethical Committee and Institutional Review Board of Peking University People's Hospital (Beijing, China) was obtained, and this study followed the tenets of the Declaration of Helsinki. Informed consent was obtained from the parents of the children.

OCT angiography

Prior to imaging, tropicamide 1% and phenylephrine hydrochloride 2.5% were used to dilate the pupils of the patients. OCTA was performed using an Optovue RTVue Avanti instrument (Optovue, Inc.). The scanning for en face angiographic visualisation included a 3×3 -mm scan pattern centred on the fovea. The superficial capillary plexus (SCP) and the deep capillary plexus (DCP) were segmented by automated module pre-set in the software. The SCP was segmented with an inner boundary $3 \mu\text{m}$ beneath the inner limiting membrane (ILM) and an outer boundary $15 \mu\text{m}$ beneath the inner plexiform layer (IPL), whereas the DCP was segmented with an inner boundary $15 \mu\text{m}$ beneath the IPL and an outer boundary $70 \mu\text{m}$ beneath the IPL. The SCP-VD and DCP-VD were automatically calculated by the software. The foveal avascular zone (FAZ) was considered the distinct avascular zone within the macula, which was automatically selected by the software. The area of the FAZ was recorded as zero if the FAZ could not be calculated by the software due to crossing vessels on the foveal centre. The area of the FAZ calculated by the software was checked by an experienced ophthalmologist. The representative OCTA image comparisons between the ROP group and the control group are shown in Fig. 1.

Optical coherence tomography (OCT)

Each participant underwent spectral domain optical coherence tomography with the same instrument. The CFT was the average value obtained from 18 radial lines and manually measured as the distance between the ILM and Bruch's membrane at the foveal centre. The inner retinal thickness (IRT) was measured manually as the distance between the inner boundary of the outer plexiform layer (OPL) and the ILM. The outer retinal thickness (ORT) was measured manually as the distance between the inner boundary of the OPL and the inner boundary of the retinal pigment epithelium.

Multifocal ERG examination

Before testing, the pupil was dilated to 8 mm with tropicamide 1% and phenylephrine hydrochloride 2.5% eye drops. Following instillation of 0.5% proparacaine, the JET electrodes were placed on both eyes and the mfERG were performed in normal room lighting. A ground electrode was

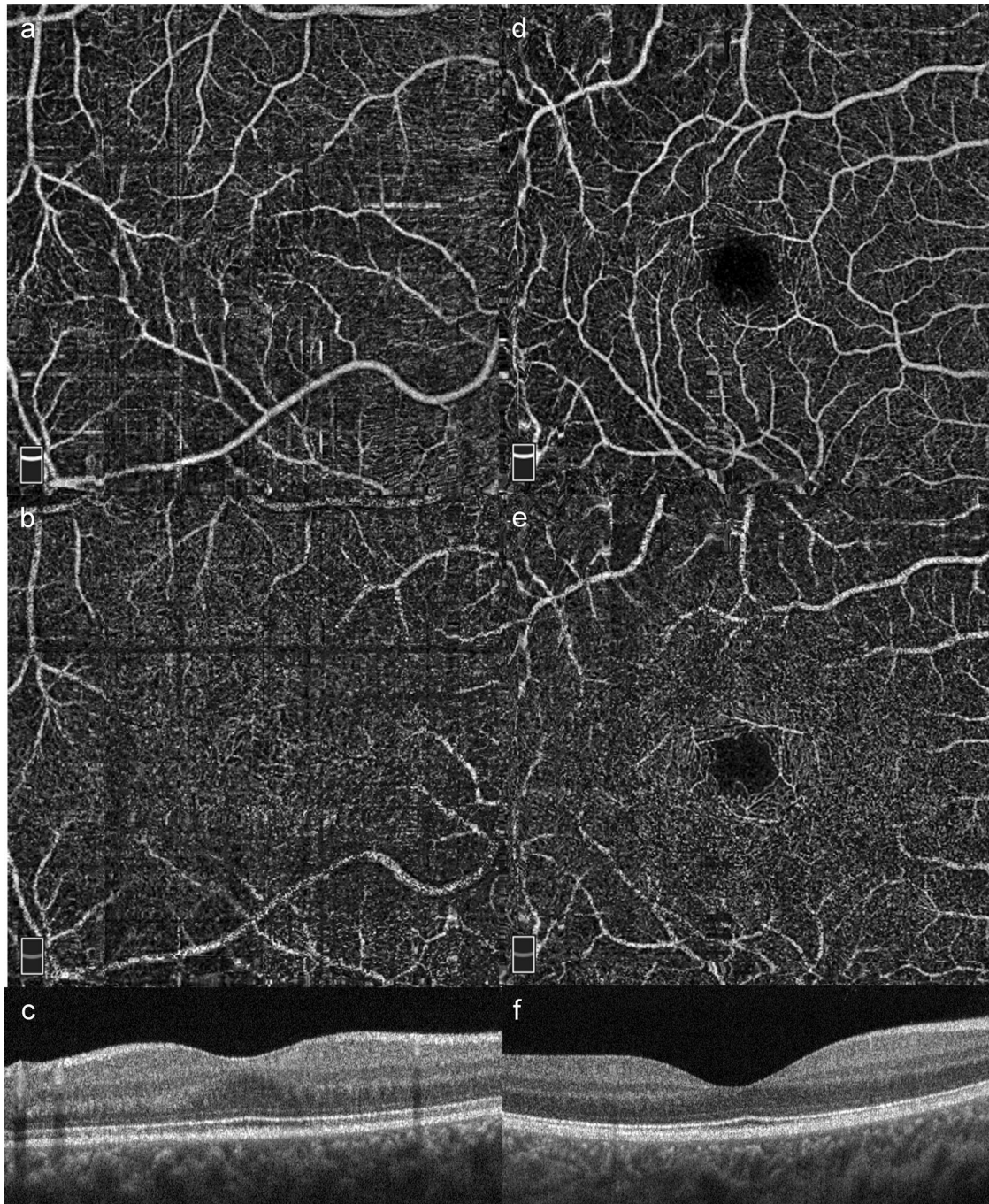


Fig. 1 Examples of optical coherence tomography angiography (OCTA) for the ROP group and control group in this study. OCTA images of foveal avascular zone (FAZ), superficial capillary plexus (SCP), deep capillary plexus (DCP), and cross-sectional OCT in the ROP group (a–c) and control group (d–f).

put on the forehead, and reference electrodes were placed on the temporal side of both eyes. During the mfERG test, the refraction was the best-corrected. To facilitate visual fixation, a small red cross with a central dot was displayed at the cathode ray tube (CRT) monitor. Fixation was monitored with the help of a camera during the test period. A protocol with a scale ray of 61 black and white hexagons

displayed on a CRT monitor was applied. The CRT frame frequency was set to 75 Hz, and 61 elements were divided into five concentric rings. The average luminance of the stimulus was set to 100 cd/m^2 , and each hexagon changed from dark to light (95% contrast) repeatedly. A 10- to 100-Hz bandpass filter was used to filter the mfERG signals. The stimulation parameters were

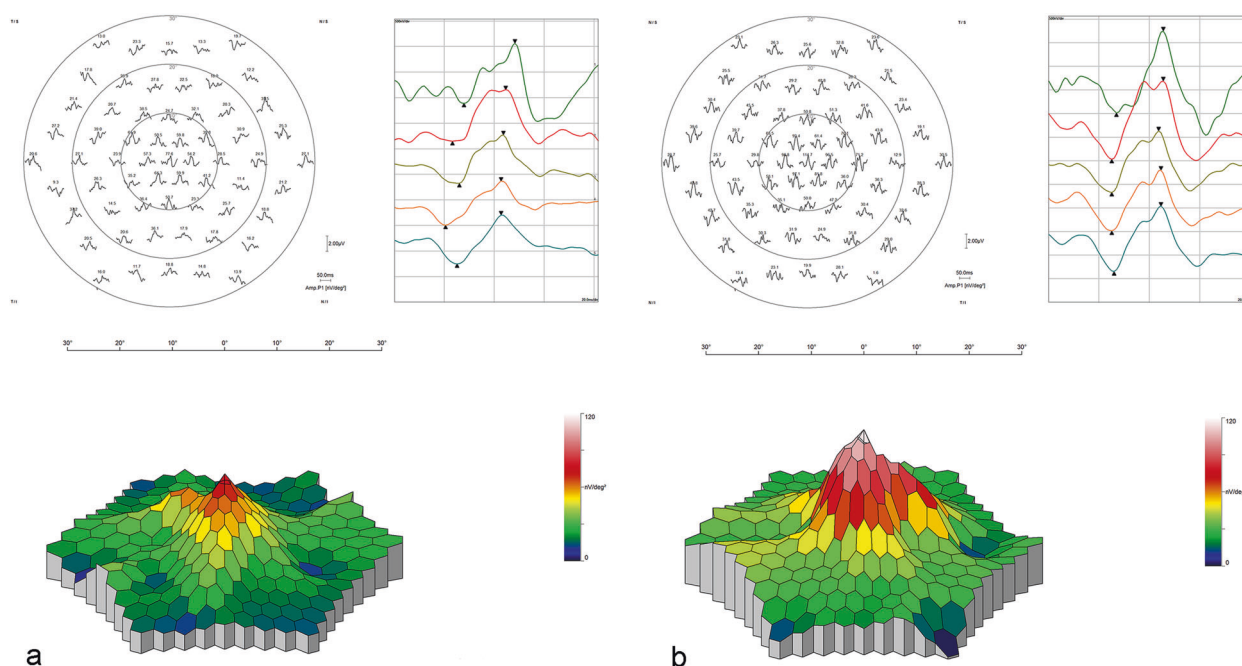


Fig. 2 Examples of multifocal electroretinogram (mfERG) results as trace arrays and colour-coded maps in this study. **a** the ROP group. **b** the control group.

based on recommendations of the International Society for Clinical Electrophysiology of Vision [14]. The mfERG responses were recorded over a period of 47 s for a minimum of eight times. The P1 amplitudes (nV/deg^2) and the P1 implicit times (ms) of the first-order kernel were recorded. Responses from representative subjects from the ROP group and the control group are shown in Fig. 2.

Statistical analysis

Statistical Packages for the Social Sciences (version 24, Chicago, Illinois, USA) was used for statistical analyses. In all analyses, a p value of <0.05 was taken to indicate a significant statistical difference. The distribution of the data was validated by the Kolmogorov–Smirnov test, which demonstrated that a high proportion of the quantitative parameters were normally distributed data (age at evaluation, amplitude of P1 in all rings of mfERG, CFT, IRT, ORT, SCP-VD and DCP-VD). Therefore, parametric test (Student's t test) was conducted for normally distributed data, and nonparametric test (Mann–Whitney test) was applied to non-normally distributed data. Fisher's exact test was used to assess the gender differences between the ROP and control groups. Relevant factors to visual acuity (in logMAR) of ROP children treated with laser photocoagulation were recognised by univariate linear regression and multivariate linear analysis, including GA, BW, post-menstrual age (PMA) of treatment, OCT findings, OCTA findings and mfERG findings.

Table 1 Demographics and profiles in the ROP group and control group.

	ROP group ($n = 26$ eyes)	Control group ($n = 29$ eyes)	p
No. patients	15	15	
Sex M/F	8/7	8/7	1.0
Age (years)	7.73 ± 1.83	8.70 ± 1.77	0.053
BCVA in logMAR (Snellen)	0.13 ± 0.09 (20/27)	0.01 ± 0.44 (20/20)	<0.001
SE (dioptries)	-1.45 ± 3.98	-1.28 ± 1.86	0.299

ROP retinopathy of prematurity, BCVA best-corrected visual acuity, LogMAR logarithm of the minimum angle of resolution.

Results

In total, 55 eyes of 30 children were included in this study. Twenty-six eyes of 15 former preterm children and 29 healthy eyes of 15 children were included. The means and standard deviations of the continuous demographic and clinical characteristics are shown in Table 1. In the ROP group, the mean GA was 30.57 ± 2.08 weeks (range: 28–32 weeks). The mean BW was 1318.46 ± 273.01 g (range: 820–1800 g). All the eyes were diagnosed with stage 3 ROP. Among them, 24 eyes had zone II ROP, while the other two eyes had zone I ROP. All children with ROP were treated with laser photocoagulation as the only treatment. The mean PMA at the time of laser photocoagulation was 39.48 ± 5.25 weeks (range:

Table 2 The comparison of structural OCT findings, OCTA findings and mfERG findings between the ROP and control group.

	ROP group (<i>n</i> = 26 eyes)	Control group (<i>n</i> = 29 eyes)	<i>p</i>
FAZ area (mm ²)	0.07 ± 0.08	0.27 ± 0.10	<0.001
SCP-VD (%)	29.89 ± 8.75	19.65 ± 8.12	<0.001
DCP-VD (%)	46.09 ± 7.39	34.66 ± 8.07	<0.001
CFT (μm)	258.77 ± 34.59	203.59 ± 21.01	<0.001
IRT (μm)	42.46 ± 26.943	9.21 ± 7.96	<0.001
ORT (μm)	216.31 ± 23.34	194.38 ± 21.28	0.001
P1 amplitude (nV/deg ²)			
Ring 1	91.76 ± 30.45	140.95 ± 39.36	<0.001
Ring 2	54.46 ± 14.63	76.78 ± 21.20	<0.001
Ring 3	35.97 ± 9.06	53.54 ± 11.37	<0.001
Ring 4	25.11 ± 7.30	33.50 ± 6.27	<0.001
Ring 5	17.68 ± 5.63	24.13 ± 5.77	<0.001
P1 implicit time (ms)			
Ring 1	45.94 ± 3.64	46.04 ± 3.07	0.747
Ring 2	44.77 ± 2.59	44.04 ± 2.49	0.319
Ring 3	44.20 ± 1.91	42.93 ± 1.90	0.014
Ring 4	43.88 ± 1.40	42.19 ± 1.55	<0.001
Ring 5	43.99 ± 0.98	42.95 ± 1.57	0.001

ROP retinopathy of prematurity, FAZ foveal avascular zone, SCP-VD superficial capillary plexus-vessel density, DCP-VD deep capillary plexus-vessel density, CFT central foveal thickness, IRT inner retinal thickness, ORT, outer retinal thickness.

34–55.1 weeks). There were no statistically significant differences observed between the patients with ROP and the controls in terms of age (7.73 ± 1.83 years old and 8.70 ± 1.77 years old, respectively, $p = 0.053$) and sex (53.3% and 53.3% males, respectively, $p = 1.0$). The mean SE of refractive error was not significantly different between the ROP and control groups (-1.45 ± 3.98 and -1.28 ± 1.86 dioptres, respectively, $p = 0.299$). The mean BCVA was significantly worse in the ROP group than in the control group (20/27; 0.13 ± 0.09 logMAR vs. 20/20; 0.01 ± 0.44 logMAR, respectively, $p < 0.001$). The movement of eyes was unrestricted in nine viewpoints, and the eyes were properly aligned in all children by performing eye cover tests. Nystagmus was not found.

Table 2 presents the comparison of the parameters generated by structural OCT, OCTA and mfERG between the ROP group and the control group. On OCTA examination, a distinct FAZ was absent in ten eyes (38.5%) in the ROP group; however, it was present in all the control eyes (100%). The mean area of the FAZ was significantly smaller in the ROP group than in the control group

(0.28 ± 0.10 vs. 0.75 ± 0.97 mm², respectively, $p < 0.001$). The mean SCP-VD and DCP-VD were significantly increased in the ROP group compared to the control group ($29.89 \pm 8.75\%$ vs. 19.65 ± 8.12 , respectively, $p < 0.001$, for the SCP-VD; $46.09 \pm 7.39\%$ vs. $34.66 \pm 8.07\%$, $p < 0.001$, respectively, for the DCP-VD).

On structural OCT examination, the mean CFT was significantly higher in the ROP group than in the control group (258.77 ± 34.59 vs. 203.59 ± 21.01 μm, respectively, $p < 0.001$). Similarly, the mean IRT and ORT were higher in the ROP group than in the control group (42.46 ± 26.943 μm vs 9.21 ± 7.96 μm, respectively, $p < 0.001$, for IRT; 216.31 ± 23.34 μm vs 194.38 ± 21.28 μm, respectively, $p = 0.001$, for ORT).

On mfERG examination, the mfERG measurements in the ROP group and the control group are presented in Table 2. The P1 amplitudes in all retinal regions were significantly smaller in the ROP group than in the control group ($p < 0.001$). There was no significant difference between the two groups in implicit times in ring 1 and ring 2 ($p > 0.05$).

In the ROP group, regarding the demographic data, all the examination parameters were not significantly correlated with GA, BW or PMA (all $p > 0.05$). The mean area of the FAZ was significantly negatively correlated with the CFT ($r = -0.630$, $p = 0.001$) and the IRT ($r = -0.651$, $p < 0.001$) but was not associated with the ORT ($r = -0.182$, $p = 0.374$). In contrast, the SCP-VD and DCP-VD had significant positive correlations with the CFT ($r = 0.490$, $p = 0.010$, for the SCP-VD; $r = 0.661$, $p < 0.001$, for the DCP-VD) and the IRT ($r = 0.589$, $p = 0.002$, for the SCP-VD; $r = 0.674$, $p < 0.001$, for the DCP-VD) but were not associated with the ORT ($r = 0.053$, $p = 0.796$, for the SCP-VD; $r = 0.201$, $p = 0.324$, for the DCP-VD). The P1 amplitude and implicit time in ring 1 were not significantly correlated with the other parameters (all $p > 0.05$).

Relevant factors to the visual acuity of ROP children with a history of laser photocoagulation were determined by regression analysis. As demonstrated by the univariate analysis, the LogMAR BCVA showed a negative correlation with PMA ($p = 0.022$), the area of the FAZ ($p = 0.066$), the SCP-VD ($p = 0.029$) and the DCP-VD ($p = 0.026$) but was positively associated with the CFT ($p = 0.048$) and the IRT ($p = 0.042$) (Table 3). Factors obtained from the univariate analysis were used to conduct a multivariable linear regression analysis. Multivariable linear regression analysis demonstrated that LogMAR BCVA was negatively related to PMA and positively correlated with the SCP-VD and the CFT ($R^2 = 0.529$, $p < 0.001$, 0.043 and 0.020, respectively, Table 3) meaning that later onset of ROP, thicker retina, and denser superficial microvasculature were associated with decreased vision.

Table 3 Univariate and multivariate regression analysis for factors correlated with BCVA (in logMAR) $R^2 = 0.529$.

	Univariate coefficient	<i>p</i>	Multivariate coefficient	<i>p</i>
GA	−0.011	0.959		
BW	−0.203	0.319		
PMA	−0.447	0.022	−0.629	<0.001
FAZ area	−0.366	0.066		
SCP-VD	−0.428	0.029	0.339	0.043
DCP-VD	−0.436	0.026		
CFT	0.391	0.048	0.409	0.020
IRT	0.402	0.042		
ORT	0.115	0.574		
P1 amplitude	−0.173	0.397		
P1 implicit time	−0.304	0.131		

GA gestational age, BW birth weight, PMA post-menstrual age, FAZ foveal avascular zone, SCP-VD superficial capillary plexus-vessel density, DCP-VD deep capillary plexus-vessel density, CFT central foveal thickness, IRT inner retinal thickness, ORT, outer retinal thickness.

Discussion

In the present study, comparisons were made in terms of the foveal structure, function, and microvascular morphology between eyes in the ROP group treated with laser photocoagulation and eyes in the control group using OCTA and mfERG. Recently, OCTA has been applied to evaluate the FAZ and vessel density in several studies. Similar to previous studies [10–13], significantly smaller FAZs and higher central foveal vessel densities in eyes with ROP were observed in this study. Chen et al. [13] concluded that there were significantly smaller FAZs and higher foveal vessel densities in ROP children previously treated with anti-VEGF, which were correlated with GA and BW. In this study, none of the examination parameters were significantly correlated with GA and BW. Nonobe et al. [11] observed a smaller FAZ and abnormal vascular density in children with a history of laser- or cryopexy-treated ROP compared to controls. Although similar results were obtained in our study, all of the children with ROP included were treated with laser photocoagulation only. Similar to our study, Falavarjani et al. [12] compared eyes with ROP treated by laser photocoagulation with control eyes. Their results indicated smaller FAZs (0.02 vs. 0.07 mm²) and larger SCP-VDs (41.8% vs. 29.9%) compared with our study.

In our study, mfERG was further used to evaluate foveal function. The P1 amplitude of ring 1 was smaller in the ROP group compared to the age- and sex-matched controls, and there was no difference in implicit time in ring 1 in the ROP group, which was consistent with the results obtained

by Michalczuk et al. [15] and Akerblom et al. [16]. Nevertheless, Fulton et al. [17] concluded that the P1 implicit time in ring 1 was longer in the ROP subjects than in the controls. Cone-driven bipolar cells are the main contributors to mfERG responses [18]. Centrifugal movement of the inner retinal neurons includes the centrifugal displacement of the cone-driven bipolar cells. In our study, the IRT was significantly higher in the ROP group than in the control group, which may indicate that the centrifugal displacement of the bipolar cells was arrested due to prematurity. The hindered process of the centrifugal displacement of the bipolar cells may provide a reasonable explanation for the lower P1 amplitude. In previous reports [16, 17, 19], responses were recorded with an array of 103 hexagons. Although a protocol with an array of 103 hexagonal elements will improve the spatial resolution of the test [14], increasing the number of stimulus elements will prolong the duration of the recording. In our study, the mean age of the children with ROP was 7.7 years old, which was younger than that previously reported (10.9–15.6 years old) [15–17, 19]. To reduce the test time and obtain high-quality images, a protocol with a scale ray of 61 black and white hexagons was used in our study.

The development of the foveal structure and vessels is a highly complicated process [20–23]. Retinal vessels start to develop from 24 to 28 weeks post conception from the optic disc towards the fovea [24, 25]. In previous histologic studies, there were two theories on the formation of the FAZ. Engerman [26] and Springer and Hendrickson [27] found that the macular capillaries in primates ceased to proliferate before reaching the edge of the fovea. Several previous reports demonstrated that antiproliferative and/or antiangiogenic factors expressed within the central foveal region hinder capillaries from growing into the fovea, resulting in the formation of the FAZ [23, 28, 29]. In contrast, Henkind et al. [30] reported that in cats and the rhesus monkeys, the fovea is fully vascularises in the foetal period, and vascular remodelling results in the formation of a distinct FAZ. Our study would seem to lend support to Henkind's hypothesis, as a smaller FAZ area and higher vascular density were observed in the ROP group treated with laser photocoagulation than in the controls, and we suggest that the apoptotic process to form the FAZ could be arrested because of prematurity.

There are two crucial steps in the formation of the foveal pit: centrifugal displacement of the inner retinal neurons and centripetal displacement of the photoreceptors [20, 22]. A major challenge is to identify the potential mechanisms that cause the displacement of different neurons. Initially, cellular displacement was considered an active process, or the neurons were attracted by molecular factors [31, 32]. However, such explanations remain unsubstantiated, as there were no specific factors

discovered in promoting different differentiated retinal neuron movement. Springer and Hendrickson [21] hypothesised that the absence of vasculature makes the inner retinal layer of the fovea quite transformable and that two intrinsic mechanical forces, intraocular pressure and retinal stretch, contribute to creating the foveal pit. In this study, the mean areas of the FAZ, SCP-VD and DCP-VD were correlated with the CFT and IRT but were not associated with the ORT, which strongly indicates that the foveal microvasculature might play a key role in the formation of the foveal pit. It was hypothesised that there was a close association between the FAZ, foveal vascular density, CFT and IRT, and the development of the foveal structure and foveal vessels were interdependent.

In this study, visual acuity was suboptimal in the ROP group compared to the controls. We further evaluated the correlations between visual acuity and foveal structure, function, and microvascular morphology in school-age children with laser-treated ROP and full-term age- and sex-matched controls. The visual outcomes related to the structural changes remain controversial. As argued by some authors, such structural changes do not correlate with visual acuity [33]. In our study, it was observed that a larger CFT was associated with worse visual acuity, which was supported by previous studies [2, 6, 34]. It was observed that the SCP-VD was associated with suboptimal visual acuity in this study. Shao et al. [35] reported similar results obtained from an animal model. We found that PMA was another independent predictor of the final visual acuity. PMA was positively correlated with visual acuity. In our study, most patients were classified into zone 2 and type 1 ROP, except for two children who had zone 1 ROP. All children with ROP received laser photocoagulation within 2 days after diagnosis. Therefore, it was hypothesised that later onsets of ROP would lead to relatively better visual outcomes. Although correlations between the foveal parameters and visual acuity have been assessed by previous studies [13, 36], this study is still thought to be the first to take the OCT, OCTA and mfERG parameters into consideration.

The following study limitations should be considered. First, we only enrolled children with ROP treated with laser photocoagulation and compared them with controls. It would be more convincing if we included children born prematurely without ROP or children with untreated ROP. The CFT and foveal function may be different between the children who received laser treatment and the children who do not receive treatment and experienced spontaneous regression [37]. Second, a subgroup analysis was not performed in terms of the ROP severity. In the ROP group in our study, 24 eyes had zone II ROP, while the other two eyes, ROP was localised in zone I. The different severities may be relevant to the degree of foveal

microvascular, structural abnormalities and foveal function. Third, we enrolled a relatively small number of cases, leading to lower power. Finally, we did not analyse the longitudinal data of each case. Iafe et al. [38] claimed that the SCP-VD and DCP-VD decrease with increasing age, while the area of the FAZ increases with age. It is important to analyse the changes in the SCP-VD, the DCP-VD and the area of the FAZ as children grow. Additional studies may be more helpful to elucidate the relationship between the formation of the foveal pit and foveal vascularisation.

In conclusion, foveal structure, function and microvascular morphology are affected in prematurely born school-age children with ROP treated with laser photocoagulation in comparison with peers born at an appropriate GA. Foveal structure, function and microvascular morphology seem to be associated with impaired visual function. Further longitudinal studies with a larger sample size are necessary to demonstrate these morpho-functional correlations over time.

Summary

What was known before

- ROP is classified as a vasoproliferative disorder and can affect the central retina, which has a possibility to lead impaired visual acuity and visual sensitivity. A few studies have focused on the foveal microvascular abnormalities in school-age children with ROP by OCTA. Previous studies have indicated that the central retinal function was impaired in school-age children with ROP as compared to children born at term using mfERG. OCT, OCTA and mfERG were applied to evaluate microstructural abnormalities, microvascular anomalies and local retinal function, respectively.

What this study adds

- Foveal structure, function and microvascular morphology are affected in prematurely born school-age children with ROP treated with laser photocoagulation in comparison with peers born at an appropriate GA. Foveal structure, function and microvascular morphology seem to be associated with impaired visual function.

Compliance with ethical standards

Conflict of interest The authors declare that they have no conflict of interest.

Publisher's note Springer Nature remains neutral with regard to jurisdictional claims in published maps and institutional affiliations.

References

- Barnaby AM, Hansen RM, Moskowitz A, Fulton AB. Development of scotopic visual thresholds in retinopathy of prematurity. *Invest Ophthalmol Vis Sci.* 2007;48:4854–60.
- Fiess A, Janz J, Schuster AK, Kolb-Keerl R, Knuf M, Kirchhof B, et al. Macular morphology in former preterm and full-term infants aged 4 to 10 years. *Graefes Arch Clin Exp Ophthalmol.* 2017;255:1433–42.
- Dubis AM, Costakos DM, Subramaniam CD, Godara P, Wirostko WJ, Carroll J, et al. Evaluation of normal human foveal development using optical coherence tomography and histologic examination. *Arch Ophthalmol.* 2012;130:1291–300.
- Hendrickson AE, Yuodelis C. The morphological development of the human fovea. *Ophthalmology.* 1984;91:603–12.
- Maldonado RS, O'Connell RV, Sarin N, Freedman SF, Wallace DK, Cotten CM, et al. Dynamics of human foveal development after premature birth. *Ophthalmology.* 2011;118:2315–25.
- Stoica F, Chirita-Emandi A, Andreescu N, Stanciu A, Zimbru CG, Puiu M. Clinical relevance of retinal structure in children with laser-treated retinopathy of prematurity versus controls—using optical coherence tomography. *Acta Ophthalmol* 2018;96:e222–8.
- Ecsedy M, Szamosi A, Karko C, Zubovics L, Varsanyi B, Nemeth J, et al. A comparison of macular structure imaged by optical coherence tomography in preterm and full-term children. *Invest Ophthalmol Vis Sci.* 2007;48:5207–11.
- Chen YH, Lien R, Chiang MF, Huang CY, Chang CJ, Wang NK, et al. Outer retinal structural alternation and segmentation errors in optical coherence tomography imaging in patients with a history of retinopathy of prematurity. *Am J Ophthalmol.* 2016;166:169–80.
- Chavala SH, Farsiu S, Maldonado R, Wallace DK, Freedman SF, Toth CA. Insights into advanced retinopathy of prematurity using handheld spectral domain optical coherence tomography imaging. *Ophthalmology.* 2009;116:2448–56.
- Balasubramanian S, Borrelli E, Lonngi M, Velez F, Sarraf D, Sadda SR, et al. Visual function and optical coherence tomography angiography features in children born preterm. *Retina.* 2018;39:2233–39.
- Nonobe N, Kaneko H, Ito Y, Takayama K, Kataoka K, Tsunekawa T, et al. Optical coherence tomography angiography of the foveal avascular zone in children with a history of treatment-requiring retinopathy of prematurity. *Retina.* 2019;39:111–7.
- Falavarjani KG, Iafe NA, Velez FG, Schwartz SD, Sadda SR, Sarraf D, et al. Optical coherence tomography angiography of the fovea in children born preterm. *Retina.* 2017;37:2289–94.
- Chen YC, Chen YT, Chen SN. Foveal microvascular anomalies on optical coherence tomography angiography and the correlation with foveal thickness and visual acuity in retinopathy of prematurity. *Graefes Arch Clin Exp Ophthalmol.* 2019;257:23–30.
- Hood DC, Bach M, Brigell M, Keating D, Kondo M, Lyons JS, et al. ISCEV standard for clinical multifocal electroretinography (mfERG) (2011 edition). *Doc Ophthalmol.* 2012;124:1–13.
- Michalczyk M, Urban B, Chrzanowska-Grenda B, Oziebło-Kupczyk M, Bakunowicz-Lazarczyk A, Kretowska M. The assessment of multifocal ERG responses in school-age children with history of prematurity. *Doc Ophthalmol.* 2016;132:47–55.
- Akerblom H, Andreasson S, Holmstrom G. Macular function in preterm children at school age. *Doc Ophthalmol.* 2016;133:151–7.
- Fulton AB, Hansen RM, Moskowitz A, Barnaby AM. Multifocal ERG in subjects with a history of retinopathy of prematurity. *Doc Ophthalmol.* 2005;111:7–13.
- Hood DC, Frishman LJ, Saszik S, Viswanathan S. Retinal origins of the primate multifocal ERG: implications for the human response. *Invest Ophthalmol Vis Sci.* 2002;43:1673–85.
- Altschwager P, Moskowitz A, Fulton AB, Hansen RM. Multifocal ERG responses in subjects with a history of preterm birth. *Invest Ophthalmol Vis Sci.* 2017;58:2603–8.
- Springer AD, Hendrickson AE. Development of the primate area of high acuity, 3: temporal relationships between pit formation, retinal elongation and cone packing. *Vis Neurosci.* 2005;22:171–85.
- Springer AD, Hendrickson AE. Development of the primate area of high acuity. 1. Use of finite element analysis models to identify mechanical variables affecting pit formation. *Vis Neurosci.* 2004;21:53–62.
- Vajzovic L, Hendrickson AE, O'Connell RV, Clark LA, Tran-Viet D, Possin D, et al. Maturation of the human fovea: correlation of spectral-domain optical coherence tomography findings with histology. *Am J Ophthalmol.* 2012;154:779–89.e2.
- Gariano RF. Special features of human retinal angiogenesis. *Eye.* 2010;24:401–7.
- Provis JM. Development of the primate retinal vasculature. *Prog Retin Eye Res.* 2001;20:799–821.
- Moskowitz A, Hansen RM, Fulton AB. Retinal, visual, and refractive development in retinopathy of prematurity. *Eye Brain.* 2016;8:103–11.
- Engerman RL. Development of the macular circulation. *Invest Ophthalmol.* 1976;15:835–40.
- Springer AD, Hendrickson AE. Development of the primate area of high acuity. 2. Quantitative morphological changes associated with retinal and pars plana growth. *Vis Neurosci.* 2004;21:775–90.
- Kozulin P, Natoli R, Bumsted O'Brien KM, Madigan MC, Provis JM. The cellular expression of antiangiogenic factors in fetal primate macula. *Invest Ophthalmol Vis Sci.* 2010;51:4298–306.
- Bohm MR, Hodes F, Brockhaus K, Hummel S, Schlatt S, Melkonyan H, et al. Is Angiostatin Involved in Physiological Foveal Avascularity? *Invest Ophthalmol Vis Sci.* 2016;57:4536–52.
- Henkind P, Bellhorn RW, Murphy ME, Roa N. Development of macular vessels in monkey and cat. *Br J Ophthalmol.* 1975;59:703–9.
- Hendrickson A, Kupfer C. The histogenesis of the fovea in the macaque monkey. *Invest Ophthalmol Vis Sci.* 1976;15:746–56.
- Provis JM, Diaz CM, Dreher B. Ontogeny of the primate fovea: a central issue in retinal development. *Prog Neurobiol.* 1998;54:549–80.
- Villegas VM, Capo H, Cavuoto K, McKeown CA, Berrocal AM. Foveal structure-function correlation in children with history of retinopathy of prematurity. *Am J Ophthalmol.* 2014;158:508–12.e2.
- Balasubramanian S, Beckmann J, Mehta H, Sadda SR, Chanwimol K, Nassisi M, et al. Relationship between retinal thickness profiles and visual outcomes in young adults born extremely preterm: The EPICure@19 Study. *Ophthalmology.* 2019;126:107–12.
- Shao Z, Dorfman AL, Seshadri S, Djavari M, Kermorvant-Duchemin E, Sennlaub F, et al. Choroidal involution is a key component of oxygen-induced retinopathy. *Invest Ophthalmol Vis Sci.* 2011;52:6238–48.
- Balasubramanian S, Beckmann J, Mehta H, Sadda SR, Chanwimol K, Nassisi M, et al. Relationship between retinal thickness profiles and visual outcomes in young adults born extremely preterm: The EPICure@19 Study. *Ophthalmology.* 2018;126:107–12.

37. Gursoy H, Bilgec MD, Erol N, Basmak H, Colak E. The macular findings on spectral-domain optical coherence tomography in premature infants with or without retinopathy of prematurity. *Int Ophthalmol*. 2016;36:591–600.
38. Iafe NA, Phasukkijwatana N, Chen X, Sarraf D. Retinal capillary density and foveal avascular zone area are age-dependent: quantitative analysis using optical coherence tomography angiography. *Invest Ophthalmol Vis Sci*. 2016;57:5780–7.